IOPscience iopscience.iop.org

Home Search Collections Journals About Contact us My IOPscience

An experimental study of the growth of Co/Pt(111) by core level photoemission spectroscopy, low-energy electron diffraction and Auger electron spectroscopy

This article has been downloaded from IOPscience. Please scroll down to see the full text article.

1994 J. Phys.: Condens. Matter 6 5025

(http://iopscience.iop.org/0953-8984/6/27/012)

View the table of contents for this issue, or go to the journal homepage for more

Download details:
IP Address: 171.66.16.147
The article was downloaded on 12/05/2010 at 18:47

Please note that terms and conditions apply.

J. Phys.: Condens. Matter 6 (1994) 5025–5038. Printed in the UK

An experimental study of the growth of Co/Pt(111) by core level photoemission spectroscopy, low-energy electron diffraction and Auger electron spectroscopy

J Thiele†‡, N T Barrett†‡, R Belkhou‡, C Guillot†‡ and H Koundi‡

† DRECAM-SRSIM, CE Saclay, 91191 Gif-sur-Yvette Cédex, France

‡ LURE, Bâtiment 209d, Centre Universitaire Paris-Sud, 91405 Orsay Cédex, France

Received 24 February 1994, in final form 14 April 1994

Abstract. We have analysed by use of synchrotron radiation induced angle resolved photoemission spectroscopy (PES), Auger electron spectroscopy (AES) and low-energy electron diffraction (LEED) the growth of ultrathin Co layers deposited at room temperature on Pt(111) surfaces. The LEED patterns indicate an incoherent epitaxy and AES data can be explained by a near layer by layer growth mode. Decomposition of the Pt $4f_{7/2}$ photoemission line shows characteristic core level shifts for the different environments of Pt atoms, giving insight concerning a relatively sharp interface structure. On the other hand, the Pt/Co interface in the Pt/Co/Pt(111) sandwich is less sharp, giving rise to two Pt surface sites. Annealing of the Co/Pt(111) system at 400 °C gives a surface alloy structure with the same symmetry and orientation as the Pt substrate.

1. Introduction

In the last few years much attention has been devoted to metallic ultrathin films, sandwiches and especially multilayers of the Co–Pt system due to its particular magnetic properties [1–7]. Their perpendicular easy axis of magnetization, important for magneto-optical recording media, is a result of the influence of the interface of the artificial layered structure [4]. Understanding the atomic and electronic structure of an interface formed by deposition of an overlayer on a single-crystal surface is the first stage in the description of the multilayer system, and resembles the high structural order in today's MBE grown superlattices. Recently, it was shown for the Co–Pt system [1] that not only the interface distances but also the crystalline orientation of the films is important for the magnetic anisotropy of artificially layered structures.

Photoemission spectroscopy (PES) experiments using synchrotron radiation have already been carried out on the Co/Pt(100) interface [3]. Using the core level shift of an atom to probe the local structural and chemical environment can give information on the lateral order of these atoms, and also about the depth profile near the surface. Thus, for Co/Pt(100) a four-monolayer-thick mixed interface was found for evaporation at room temperature. For multilayers the interdiffusion for this orientation was smaller than for the (111) direction [7]. This was determined by low-angle x-ray diffraction measurements of MBE superlattices grown with different orientations. Since for multilayer structures the (111) direction, in contrast to the (100), shows a perpendicular anisotropy [1], we have decided to study the growth of Co on this Pt surface. It should be possible to determine an upper limit for the sharpness of the interface, particularly useful for multilayer systems with epitaxial growth.

0953-8984/94/275025+14$19.50 © 1994 IOP Publishing Ltd

Recently it was shown by LEED experiments on a Co wedge grown by MBE on a Pt(111) single crystal that Co grows in incoherent epitaxy on this surface [6], i.e. the Co overlayer has the same interatomic spacing as in bulk Co but it follows the orientation of the Pt substrate. The structure of the interface was not investigated. It was not possible to determine whether interdiffusion at the interface had taken place. The Co/Pt(111) interface has also been studied by x-ray photoelectron diffraction. The present authors favour a sharp interface with ordered FCC Co layers growing in a layer by layer mode [8]. Finally a scanning tunnelling microscopy (STM) study of the same interface concludes that the growth mode is nearly layer by layer for the first three layers, after which growth proceeds in the form of three-dimensional islands [9]. Evidence is presented for an HCP Co layer. Furthermore, it is suggested that the strain relaxation in the first Co layer is activated by the second-layer Co atoms.

The understanding of the Co/Pt(111) interface is a first step in the fabrication of Pt–Co multilayer systems. The inverse interface Pt/Co(0001) also needs to be investigated. An AES and LEED study [10] suggested that the Pt grows epitaxially with an HCP structure on the Co(0001) face at room temperature. The growth proceeds by the formation of pyramidal islands with a maximum height of four monolayers (ML), above which coalescence occurs.

In this paper we present core level PES results on the growth and annealing of Co/Pt(111), and the formation of a Pt/Co/Pt(111) sandwich. The work is presented as follows. In section 2 we describe the experimental details. In section 3 we give first the AES and LEED results, which allow us to situate the PES results with respect to previous work. These results are discussed in section 4.

2. Experiment

Clean Pt(111) single-crystal surfaces were obtained by Ar ion sputtering and annealing cycles (at 650 °C) in an ultra-high vacuum (UHV) chamber with a base pressure of 1×10^{-10} Torr and checked by AES in the derivative mode and LEED. After cleaning only a small amount of C was observed by AES. A C (273 eV) peak to peak height smaller that one tenth of that of Pt (237 eV), corresponds to less than 0.06 ML C [11]. LEED showed a clear (1×1) pattern with bright, sharp spots and low background. For the LEED measurements an electron beam primary energy of 65 eV was used to optimize the surface sensitivity.

Co evaporation was carried out at room temperature by resistively heating a 99.99% pure Co wire, which increased the pressure to 1×10^{-9} Torr during evaporation. Each deposition was characterized by AES, LEED and PES. The experiment was carried out at the Super ACO synchrotron source at LURE Orsay, on the beamline SA 73b with a toroidal grating monochromator (TGM 7°) monochromator.

To study the Pt $4f_{7/2}$ photoemission line (binding energy (BE) between 71.05 eV and 71.15 eV in the bulk [3, 12]) the photon energy was set at 155 eV using p polarization, optimizing the Pt cross-section, the monochromator response and minimizing the photoelectron mean free path, to increase surface sensitivity. The analyser was set to the normal of the sample surface. With an overall energy resolution, due to monochromator and analyser, of 0.54 eV, a count rate of about 1500 cps was attained.

On thicker Co layers (5–6 ML) we have deposited some Pt (99.99%) with the same kind of source to obtain information from the reverse interface (Pt/Co) and in particular to determine the surface core level shift (SCLS) of Pt atoms at the surface in a Co rich environment.

Finally, some preliminary results on the influence of moderate *in situ* annealing (up to 400 °C) of the Co/Pt(111) system are also presented.

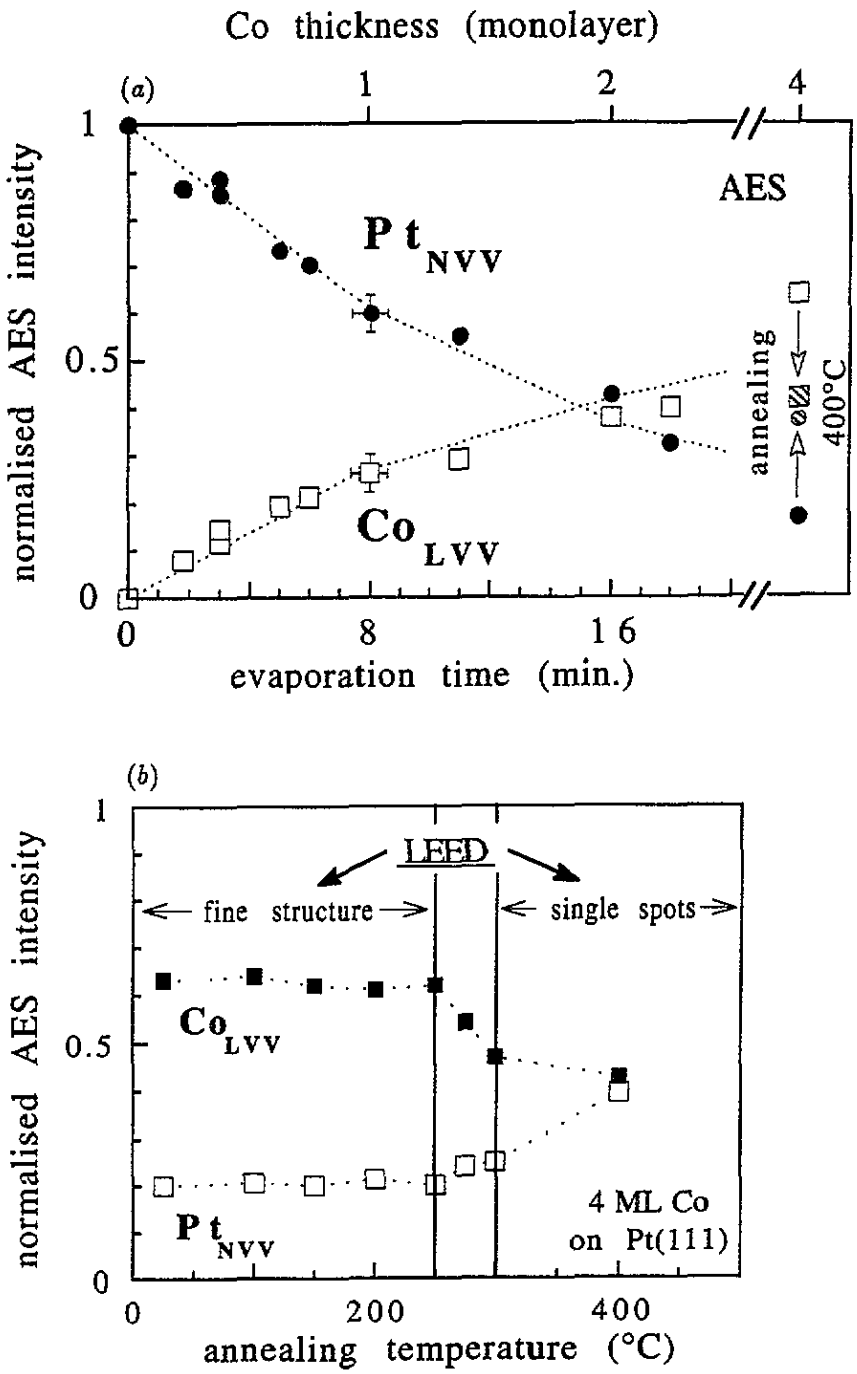

Figure 1. (*a*) The evolution of the normalized Pt NVV (64 eV) and the Co LVV (770 eV) Auger lines as a function of evaporation time. A layer by layer growth mode has been fitted using values obtained by previous authors [5]. The change in the AES intensities after annealing at 400 °C is also shown. (*b*) The temperature dependence of the Co and Pt AES signals, with the corresponding LEED patterns.

3. Results

3.1. Auger electron spectroscopy

A series of depositions at constant evaporation rate was performed. After each characterization the sample was cleaned. An identical increase of pressure during the evaporation guaranteed a steady evaporation flux. Figure 1(*a*) shows the AES intensities of the Pt NVV peak (64 eV) and the Co LVV peak (770 eV) as a function of deposition time (or Co thickness, due to the steady flux). In order to give a lower limit for the evaporation rate we have fitted the evolution of the Auger intensities with a layer by layer growth mode. For the Pt NVV intensity we have used the mean free path determined by Boeglin *et al* [5] i.e. 5 Å, which gives 1 ML after 8 min. This determines the mean free path for the Co LVV peak to be about 10 Å. Following this calibration we note that after 2 ML the experimental points agree less well with the layer by layer growth mode. Recent inelastic mean free path calculations by Tanuma *et al* [13] suggest values of 4.5 Å and 12.8 Å for the Pt and Co lines respectively. Given the uncertainty in the value of the Co intensity from an infinitely thick layer these do not significantly affect the results. Another problem with estimations of the mean free path is the role of elastic scattering. Recent work [14] shows that this is a maximum for a Co layer in the range 200–250 eV, thus we can assume that it does not play an important role in the estimation of the Co layer thickness. From the Auger intensities we can say that the Co may have to begin with a layer by layer growth mode, but we need to correlate the Auger results to those obtained with other techniques to be more precise.

Annealing the Co/Pt(111) system up to 250 °C did not change the AES intensities. For higher temperatures interdiffusion sets in, shown by an enhancement of Pt AES signal and an attenuation of the Co LVV peak. This evolution is blocked after sufficient annealing at 400 °C (see figure 1(*b*)). We have therefore measured the AES intensities for a 4 ML Co overlayer as a function of annealing time. The results are integrated into figure 1(*a*), showing the AES intensities before and after annealing at 400 °C for 1 h 15 min.

3.2. Low-energy electron diffraction

For Co coverages up to $\theta = 1.5$ ML the LEED patterns of the films do not differ from the clean Pt diagram (figure 2(*a*)). For $\theta > 1.5$ ML additional LEED spots with sixfold symmetry become visible, corresponding to the lattice spacing of Co (figure 2(*b*)). With increasing thickness the LEED pattern develops additional sixfold arrays of spots, where one of them is the initial Pt spot (figure 2(*c*)). Each sixfold array has a fine structure that goes beyond first order. Here we have to point out that even small C incorporation disturbs this sixfold fine structure and leads to large, fuzzy LEED spots. For higher coverages (> 8–9 ML) the LEED pattern loses this superstructure and has a sixfold symmetry. We have subsequently redeposited Pt onto the Co overlayer. The fine structure of the LEED pattern after Co deposition was suppressed by additional Pt evaporation, but the main spots due to the Co overlayer were still observed.

Annealing the 4 ML Co/Pt(111) sample up to 250 °C for a few minutes did not change the LEED pattern; however, the LEED fine structure is weakened with annealing time above 300 °C and a (1 × 1) pattern is recovered with fine single spots (figure 2(*d*)). The evolution of the LEED pattern as a function of annealing time is indicated in figure 1(*b*). The symmetry and orientation of the LEED diagram after annealing is the same as that of the clean Pt(111) substrate.

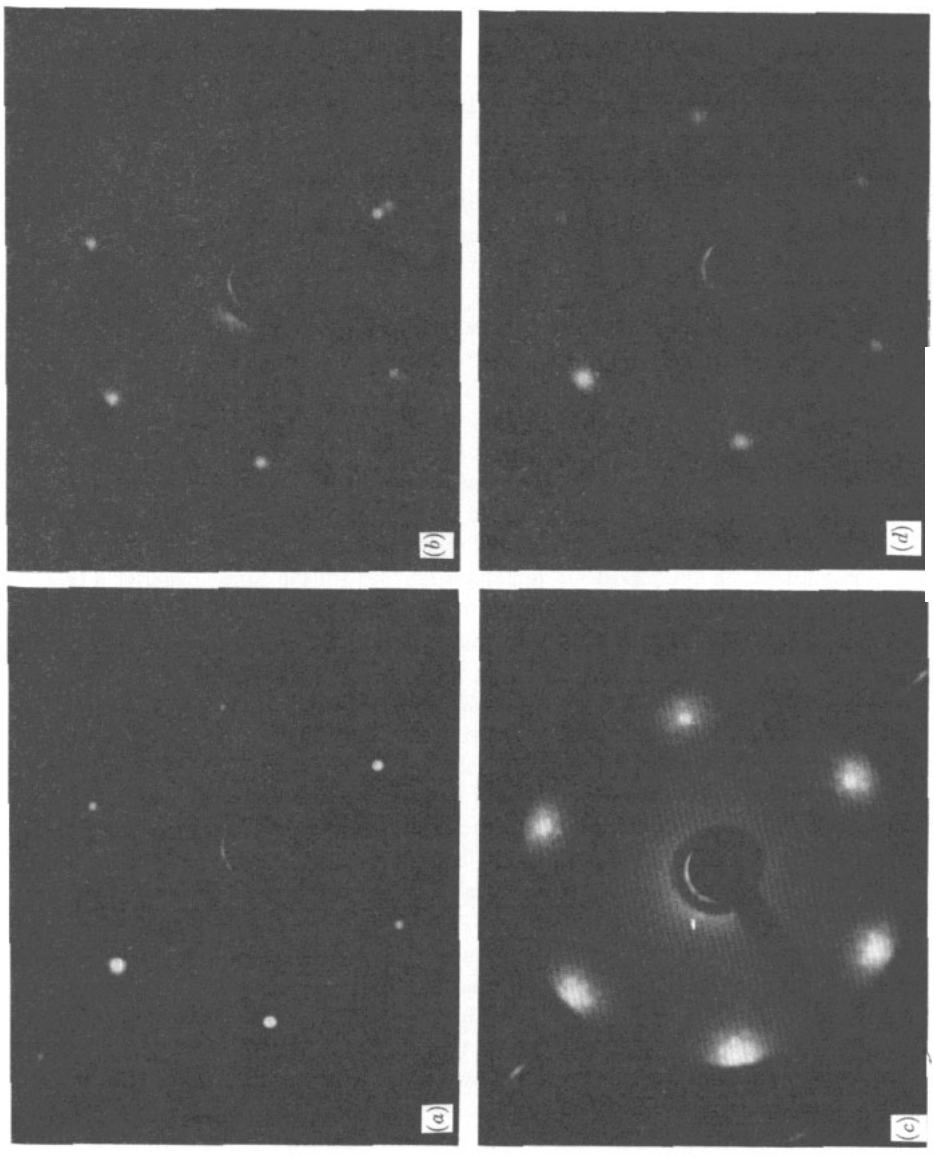

Figure 2. LEED patterns at 65 eV of the clean Pt(111) surface (*a*) and after Co deposition of 2 ML (*b*) and 5 ML (*c*). After annealing the 5 ML sample at 400 °C the pattern changes to (*d*).

3.3. Core level photoemission spectroscopy

For the analysis of the Pt $4f_{7/2}$ spectra the binding energy scale was calibrated by measuring the Fermi level for each spectrum. The signal intensity obtained from the clean Pt surface was 13 000 counts on a background of 2000. All spectra were normalized with respect to the background at constant kinetic energy (KE) on the low-BE side of the peak. The continuous background was stepped (Shirley type [15]). A Doniach–Sunjic peak shape [16] was fitted with the following parameters: asymmetry $\alpha = 0.19$; Lorentzian width $2\gamma = 0.5$ eV; overall Gaussian instrument function determined on the measured Fermi levels, 0.54 eV. The resulting positions of bulk (B) and surface (S) emission from the clean Pt substrate (figure 3) are (70.74 ± 0.03) eV and (71.13 ± 0.03) eV respectively, giving an SCLS of 390 meV, in good agreement with previous results [12] and theoretical predictions [17]. The uncertainty given is the standard deviation from the mean peak positions for the ensemble of the measured spectra, and is comparable to the uncertainty in the peak position for each fit. The main error in the determination of the peak position is introduced by the measurement of the Fermi level. Figure 3 also shows the decompositions of the spectra corresponding to 0.4–3 ML Co/Pt(111). With increasing Co coverage the overall Pt $4f_{7/2}$ intensity is reduced and the ensemble shifted to higher binding energy.

Looking more closely at the evolution of the individual peaks we observe that the clean Pt surface peak S is rapidly attenuated, falling to zero between 1 and 1.5 ML of Co. The bulk peak is not shifted but undergoes a dramatic evolution due to the increasing Co thickness. The evolution of the peak intensities as a function of deposition time is shown in figure 4. The most remarkable feature is the increase in B with respect to the intensity measured off the substrate, allied with the rapid attenuation of the clean surface peak, S.

We have continued the Co deposition beyond 4 ML and for the sake of clarity a typical spectrum is shown in figure 5. It is compared to the clean Pt substrate, and to the 4 ML Co/Pt(111) after annealing at 400 °C. For the unannealed system there is clearly a (small) peak at higher binding energy, (71.60 ± 0.05) eV, with respect to the clean Pt bulk emission. We note that after annealing we observe two peaks, one in the same position as the Pt bulk and the other at a higher binding energy, close to the small peak observed after deposition of 4 ML of Co. This second peak has been labelled B*, and has a binding energy of (71.40 ± 0.03) eV. The parameters for the analysis of this peak were slightly different from these for S and B ($\alpha = 0.11$; $2\gamma = 0.5$ eV) based on values found for sampoles of CoPt alloys [18]. The evolution of the Pt $4f_{7/2}$ peaks and the Co 3p as a function of annealing time at 400 °C is shown in figure 6(*a*). After a rapid initial change the peak intensities flatten out and appear to be stable. The Pt $4f_{7/2}$ line measured during annealing may be decomposed into two components, labelled B* and S*. The evolution of S* and B* during annealing is shown in figure 6(*b*). After an initial rapid growth both S* and B* are stable. The inset to figure 6(*b*) show in detail the behaviour of these peaks during the initial rapid stage. The intensity of B* reaches a local maximum at 30 s.

The changes in the Pt $4f_{7/2}$ spectra were measured after re-evaporating Pt onto the Co overlayer. The contribution of the Pt substrate to these spectra can be neglected due to the small mean free path of the photoelectrons. This was checked by the PES extinction of the Pt substrate signal before evaporation of Pt.

The decomposition of the Pt $4f_{7/2}$ spectra for the Pt redeposited on the Co films ($\Theta_{Co} \simeq 6$ ML) is shown in figure 7. For 0.3 ML we find two peaks near the positions of B* and S*. S* has the same binding energy as the bulk peak B of the clean Pt substrate. For coverages greater than 0.7 ML we found once again a peak similar to S at 70.81 eV.

The results of the Pt $4f_{7/2}$ decomposition during the growth of Co, the formation of a

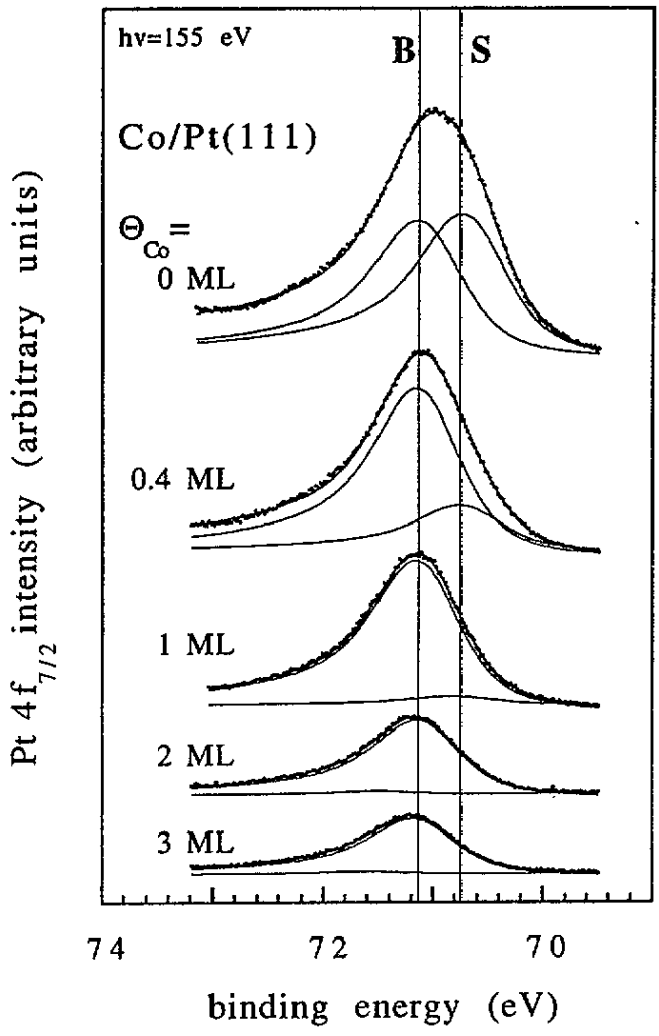

Figure 3. Examples of decomposition of the Pt $4f_{7/2}$ core level spectra of the clean Pt(111) surface and those after different Co depositions. The position of the bulk Pt line is indicated.

sandwich and the annealing of a thick Co layer are summarized in table 1. The variations in the uncertainty of the core level positions are due to the statistics of the measurements.

4. Discussion

4.1. Growth of Co/Pt(111)

We interpret these results as follows. AES suggests a growth mode that, to begin with at least, is close to a layer by layer model. This is confirmed by the LEED images for low Co coverages, which do not change with respect to the Pt surface. Thus we may imagine that at least the first Co layer grows epitaxially on the Pt substrate. The attenuation of the surface core level peak supports this idea. At the same time we measure an apparent

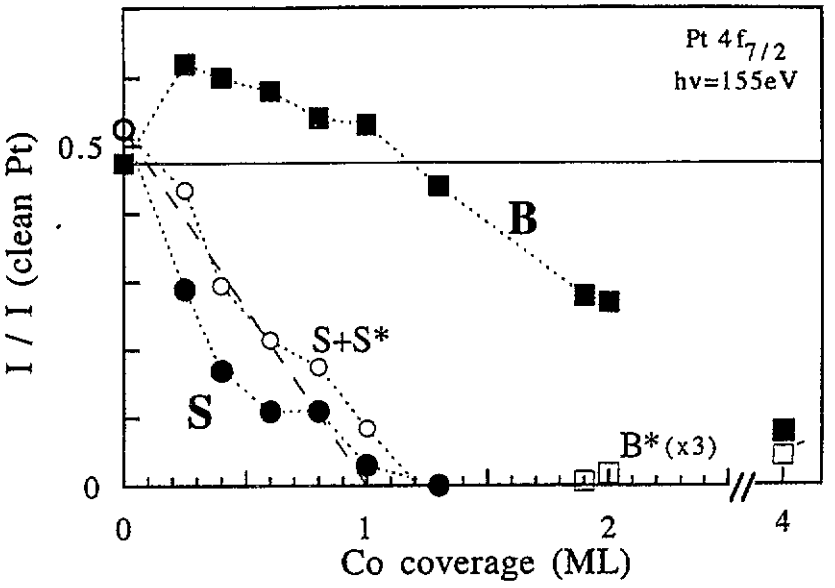

Figure 4. The intensities of the surface (S) and bulk (B) photoemission of Pt as a function of Co coverage. Both were normalized to the intensities found by decomposition of the spectra of the clean Pt(111) surface. The intensity of B> 1 is labelled S* and is added to S. This gives the total surface emission during the early stages of Co growth. The long-dashed line is an interpolation from the first values of the total surface emission.

reinforcement of the Pt bulk peak B. However, it is known from theory [18] and experiment [3, 18] that the chemical shift on the Pt $4f_{7/2}$ level due to a mixed Pt/Co environment is towards higher binding energy. If this shift is of the same order as but of opposite sign to the surface core level shift we cannot distinguish between the pure Pt bulk emission and the Pt surface emission in a mixed Co–Pt environment. Further evidence for the existence of such a peak is discussed in subsection 3.2. Thus, we interpret the rapid extinction of S as being due to, on the one hand, Pt atoms at the (111) surface that become bulk coordinated and, on the other hand, Pt surface atoms that maintain a surface coordination but have a mixed chemical environment. The latter site gives rise to a second peak, S*, which, within the resolution of the experiment has the same binding energy as the Pt bulk peak, B. As a first approximation, the real surface emission is therefore greater than the part of S and is shown as sum of (S+S*) in figure 4. S* is estimated from the increase of B in relation to the clean sample. The interpolation (dotted line in figure 5) of the surface intensity (S+S*) for the thinnest Co layers is nearly zero at 1 ML, supporting our calibration of the evaporation flux. But the persistence of S for $\Theta_{Co} = 1$ ML is evidence that there are Co atoms in the second layer before the first layer is completed. The core level intensity suggests that after depositing 1 ML of Co about 0.9 ML is in the first overlayer, the rest in the second. Such a growth mode would not significantly affect the AES intensities. The surface chemical shift of S* with respect to S is 390 meV.

For $\Theta > 1.5$ ML two LEED patterns are superimposed; the first is due to the substrate, whilst the second is due to the Co overlayer. The difference in the spot spacing corresponds to the lattice spacing difference between the bulk Co and Pt (9.4%). Thus the Co, which is nearly epitaxial for the first overlayer on the Pt, relaxes rapidly to assume the spacing found in bulk Co. Given the quasi-layer by layer growth mode this implies that the relaxation takes

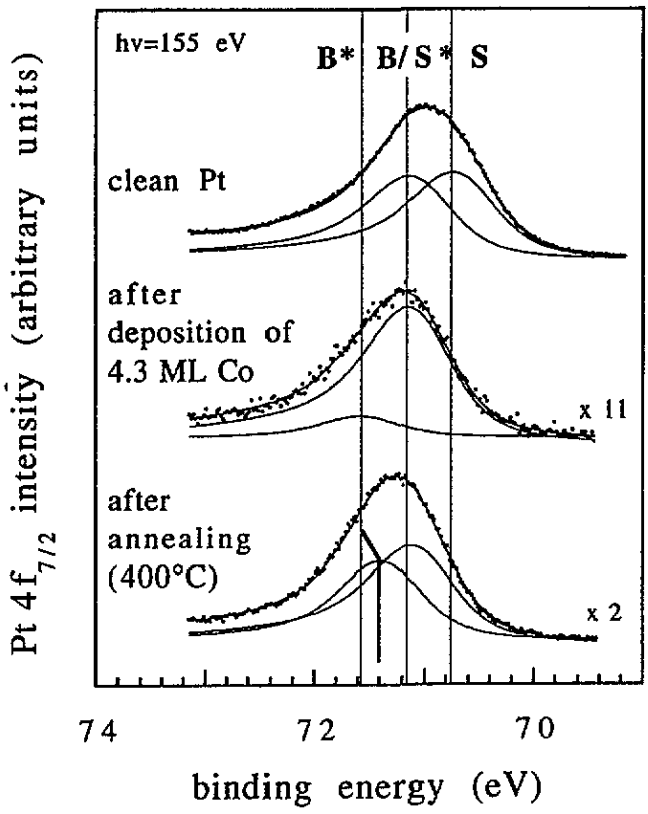

Figure 5. A comparison between the Pt $4f_{7/2}$ core level spectra for clean Pt(111), 4.3 ML Co/Pt(111) and the same system after annealing at 400 °C. Note that the peak on the high-binding-energy side of B shifts after annealing. The heavy line indicates the position of the bulk $Pt_{25}Co_{75}$ alloy peak.

place around defects in the Co surface layer. It has been suggested by STM measurements [9] that the second-layer Co atoms accommodate the strain by allowing a rearrangement of the first-layer Co atoms. This would explain the double spots observed in LEED at such a low coverage. Equally this explains the lack of interdiffusion between the Co overlayer and the Pt substrate. This is confirmed in PES by the single bulk peak. Such a growth mode is known as incoherent epitaxy.

Above 3 ML the LEED pattern changes dramatically and a sixfold fine structure appears around each spot. Like previous authors we interpret this as a modulation of the Co LEED pattern by the substrate [6]. The nth order of the fine structure is given by $2\pi n(1/a_{Co}-1/a_{Pt})$ where a_{Co} and a_{Pt} are the lattice parameters of Co and Pt, respectively. We exclude the possibility of a Moiré pattern since the fine structure goes beyond first order, unlike the conclusion drawn by Grütter and Durig [9]. What is interesting is the appearance of B*, which can only be due to a second bulk site, shown in figure 4 for Co overlayers above 2 ML. This may indicate that the rearrangement of the first-layer Co atoms, which essentially eliminates the defects necessary for the initial epitaxial growth, permits some of the Pt surface atoms to penetrate the first Co overlayer. These atoms are then in a very Co rich environment, richer than for those that stay in the first layer of the substrate (nine Co neighbours compared to three) and therefore the core level is shifted by 470 meV to higher

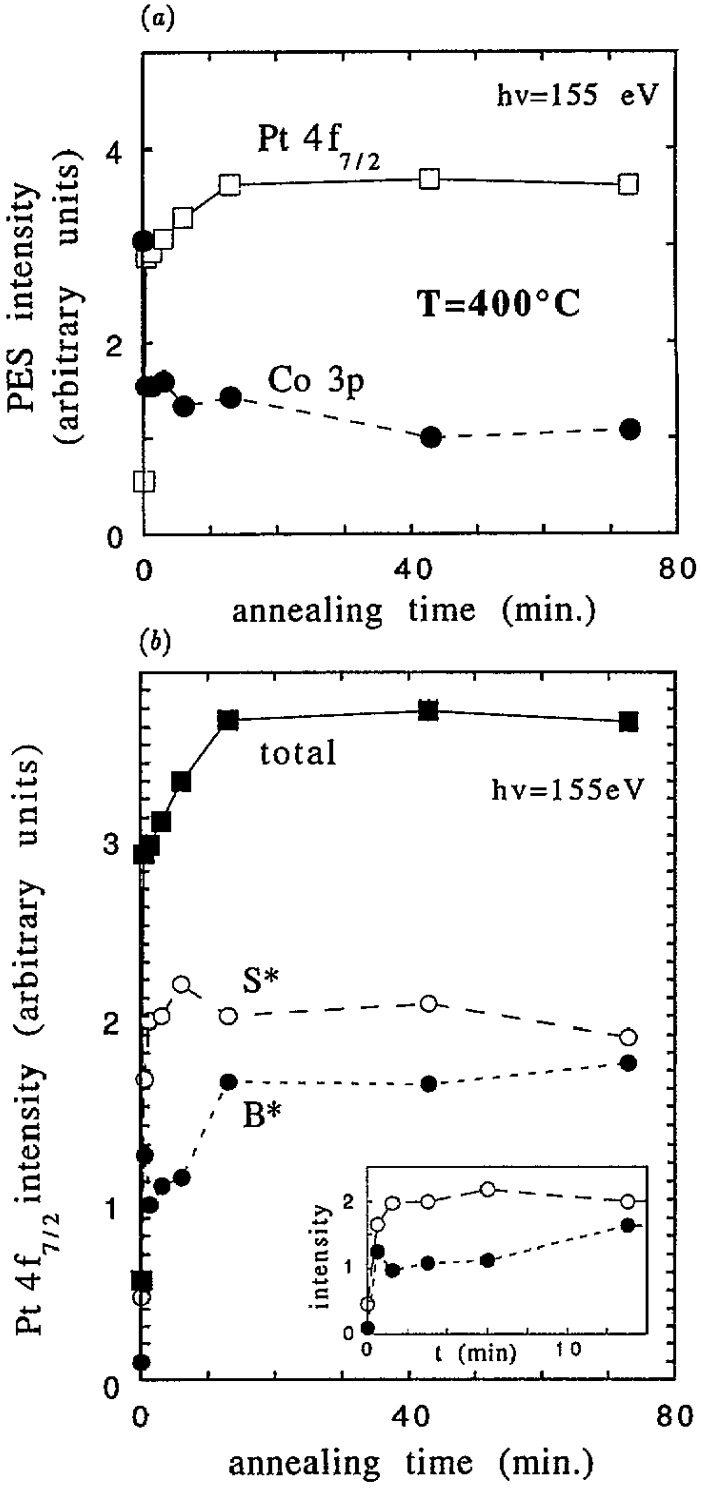

Figure 6. (*a*) The evolution of the Pt $4f_{7/2}$ and Co 3p core levels as a function of annealing time at 400 °C. (*b*) The evolution of the surface and bulk alloy peaks, S* and B*, as a function of annealing time. The details of the initial rapid dissolution are shown in the inset.

Table 1. The binding energy (in electronvolts) of the $4f_{7/2}$ level of Pt: in a Pt rich environment (at the surface S, in the bulk B), at the surface with Co neighbours (S*) and in a Co rich environment in the bulk (B*). The core level shifts (in millielectronvolts) relative to the pure Pt bulk value B are given in parentheses.

	S	B	S*	B*
Co/Pt(111)	70.74 ± 0.07 (−390)	71.13 ± 0.05	—	71.60 ± 0.05 (+470)
Pt/Co/Pt(111)	70.81 ± 0.03 (−320)	—	71.13 ± 0.03 (±0)	71.56 ± 0.04 (+430)
Co/Pt(111) after annealing	—	—	71.08 ± 0.05 (−50)	71.40 ± 0.05 (+270)

binding energies. This interpretation is confirmed by comparison with the spectrum obtained on the same system after annealing at 400 °C, and by the core level shifts measured on the bulk $Pt_{25}Co_{75}$ alloy [18]. In the former case we form a surface alloy (see subsection 4.3); in the latter we measure the core level shift due to the alloy environment in thermodynamic equilibrium. Both display a chemical shift towards higher binding energy.

We may estimate the number of Pt atoms involved in this rearrangement from the intensity of B*, taking account of the attenuation due to the Co overlayer. Neglecting photoelectron diffraction effects we conclude that up to 0.1 ML of Pt participate in the relaxation of the first Co layer and hence have a Co rich environment. To check whether it is reasonable to neglect photoelectron diffraction effects on the electrons emitted by the substrate we have plotted the Pt AES intensity as a function of the Pt core level intensity in figure 8. The former has little angular resolution, whereas the latter has an angular resolution of about 2°. We obtain a straight line, which indicates that the Co overlayer does not introduce important anisotropies in the substrate emission. This is to be expected for incoherent epitaxial growth of Co on the Pt substrate. The principal crystallographic axes of the Co overlayer and the Pt substrate are no longer aligned and therefore the forward scattering effects, which could give rise to an important anisotropy in the photoemission signal, become negligible.

4.2. Pt/Co/Pt(111) sandwich

When we redeposit Pt onto the Co overlayer the picture changes. If the second Pt/Co interface were sharp we would expect the inverse evolution of the Pt $4f_{7/2}$ emission with respect to that observed for Co/Pt(111). Instead, we observe first a surface peak S* for low Pt coverages, and above 0.7 ML we observe the appearance of a surface peak corresponding to the clean Pt surface, S. The LEED pattern indicates that the structure of the Co overlayer remains unchanged, but in PES we clearly measure a different chemical environment. This fits rather nicely with the results of the STM work on Co overlayers greater than 3 ML, which suggested that the growth mode became island like, whilst respecting the hexagonal Co structure. This would give rise to triangular pits and bumps at the overlayer surface with a peak to valley distance of up to 6–7 ML. Thus, the first Pt atoms arriving at such a surface will preferentially occupy sites at the base of the triangular pits, and thus be in a Co rich environment, explaining the alloy shift of 390 meV. Rapidly these sites will be occupied and subsequent Pt atoms will have an environment similar to that at the clean Pt(111) surface. Further Pt deposition gives rise to bulk Pt positions. The LEED pattern measured after sandwich formation does not revert to the threefold symmetric Pt(111) pattern. This supports the idea that the Pt grows with an HCP structure on the Co [10].

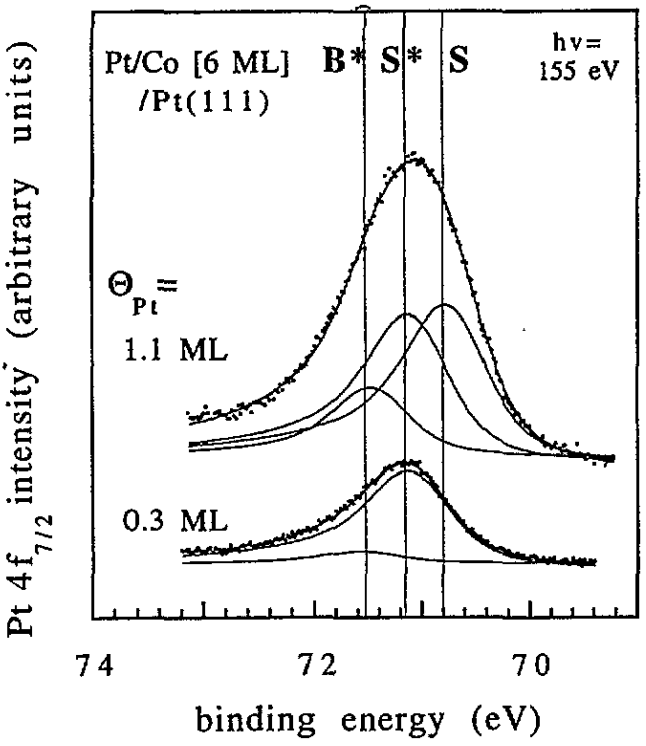

Figure 7. The decomposition of the Pt $4f_{7/2}$ core level spectra from Pt evaporated on about 6 ML thick Co films on Pt(111).

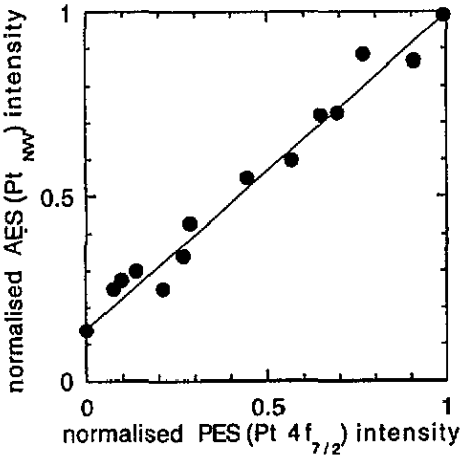

Figure 8. The relation between the angle resolved Pt $4f_{7/2}$ photoemission (PES) signal and the Pt NVV (64 eV) Auger (AES) intensity. Both are normalized to the intensity of the clean sample.

4.3. Annealed Co/Pt(111)

The temperature dependence of the Pt and Co AES signals and the LEED patterns demonstrate that for temperatures below 250 °C the structure of the incoherent epitaxial layer of Co/Pt(111) is maintained and no interdiffusion takes place. Above 300 °C this changes and after annealing the AES Pt signal increases whilst the Co intensity decreases see figure 1(*b*).

This evolution is initially very fast, but for annealing times longer than 10 min the AES intensities remain stable. Thus the interdiffusion is blocked. The core level spectra measured after annealing for 1 h 15 min at 400 °C show two Pt peaks, S* (or B) and B* (see figure 5). The first remark to be made is that the dissolution kinetics do not behave as for a classical dissolution process following Fick's law. As can be seen from figure 6 the first stage is extremely fast, followed by a blocking of the dissolution. This is very reminiscent of the results observed on the Pt/Cu(111) system [19], leading to the formation of a surface alloy. The dissolution of the overlayer is blocked by the local equilibrium established between surface segregation and the formation of an alloy in the bulk [19, 20]. In the case of the annealed Co/Pt(111) system S* and B are indistinguishable, hence the core level spectra could also be explained qualitatively by the formation of an extended interface in the bulk, giving rise to two peaks, B and B*. However, this interpretation may be excluded since the number of atomic layers probed in PES is far less than the number required to fit the relative intensities measured after annealing. We interpret the spectra taken after annealing as indicative of the formation of a surface alloy over several monolayers, sufficient to extinguish the Pt bulk signal. Since B* is close to the position measured for the bulk $Pt_{25}Co_{75}$ alloy [18], and the initial Co overlayer is about 4 ML thick, we may estimate that the surface alloy extends over some 16 ML. The alloy is formed by penetration of Co into the Pt substrate, demonstrated by the same symmetry and orientation observed by LEED on the Pt(111) surface and the alloy surface. The formation of a Pt–Co surface alloy will be presented in greater detail in a future paper.

4.4. Pt/Co magnetic multilayers

It is worthwhile commenting on the implications of these results. The relatively sharp Co/Pt(111) interface is important in obtaining a magnetic anisotropy, since interdiffusion reduces the magnetic moment of the Co layer [6]. These authors have also measured the vertical magnetic anisotropy of a Co thin film on Pt(111) and find a maximum at 3 Å. With increasing thickness the magnetic moment rotates and for thick Co layers it is in the surface plane. Structural investigations of the Co film have proved difficult. The coherence length of small-angle x-ray scattering is of the same order as the Co film thickness. Thus core level PES measurements and photoelectron diffraction can give useful information on the layer structure. The roughening of the Co overlayer after about 3 ML may also have an important effect on the possible magnetization of the film. This also means that the Pt/Co interface is less sharp than the Co/Pt(111) interface. We need to investigate the Pt/Co/Pt(111) growth mode, above all to see in which conditions, if at all, it is possible to reproduce the incoherent epitaxy of Co in a multilayer structure. PES measurements are under way to study this. Secondly, the surface alloy presents some potentially novel possibilities. It would be interesting to fabricate a Co/Co–Pt multilayer, which may allow a less incoherent epitaxy, thus sharpening the Co/Co–Pt interface and providing a new magnetic system.

5. Conclusions

We have studied the early stages of Co/Pt(111) growth and the formation of a Pt/Co/Pt(111) sandwich at room temperature using AES, LEED and core level PES. Co grows in incoherent epitaxy on the Pt(111) surface, giving a sharp interface. The strain relaxation of the first Co layer may concern a fraction of the Pt interface atoms. Above 3 ML the Co overlayer grows as islands. The atomically rough Co surface gives rise to a rougher Pt/Co interface than for Co/Pt(111). Annealing the Co/Pt(111) system at 400 °C results in the formation of a Pt–Co surface alloy, with a stoichiometry close to that of $Pt_{25}Co_{75}$.

References

[1] Lin C-J, Gorman G L, Lee C H, Farrow R F C, Marinero E E, Do H V, Notarys H and Chien C J 1991 *J. Magn. Magn. Mater.* **93** 194

[2] Zeper W B, van Kesteren H W, Jacobs B A J, Spruit J H M and Carcia P F 1991 *J. Appl. Phys.* **70** 2264

[3] Boeglin C, Carrière B, Deville J P, Scheurer F, Guillot C and Barrett N 1992 *Phys. Rev.* B **45** 3834

[4] den Broeder F J A, Hoving W and Bloemen P J H 1991 *J. Magn. Magn. Mater.* **93** 562

[5] Boeglin C, Barbier A, Carrière B, Cousandier R, Deville J P, Scheurer F and Speisser C 1991 *Surf. Sci.* **1251/252** 602

[6] McGee N W E, Johnson M T, de Vries J J, and aan de Stegge J 1993 *J. Appl. Phys.* **73** 3418

[7] Lee C H, Farrow R F C, Lin C J and Marinero E E 1990 *Phys. Rev.* B **42** 11 384

[8] Galeotti M, Atrei A, Bardi U, Cortigiani B, Rovida G and Torrini M 1993 *Surf. Sci.* **297** 202

[9] Grütter P and Dürig U T 1993 *Phys. Rev.* B submitted

[10] Barbier A 1993 *PhD Thesis* Strasbourg

[11] Biberian J P and Somorjai G A 1979 *Appl. Surf. Sci.* **2** 352

[12] Belkhou R, Barrett N T, Guillot C, Barbier A, Eugène J, Carrière B, Naumovic D and Osterwalder J 1993 *Appl. Surf. Sci.* **65/66** 63

[13] Tanuma S, Powell C J and Penn D R 1991 *Surf. Interface Anal.* **17** 911

[14] Jablonski A, Jansson C and Tougaard S 1993 *Phys. Rev.* B **47** 7420

[15] Shirley D A 1972 *Phys. Rev.* B **5** 4709

[16] Doniach S and Sunjic M 1970 *J. Phys. C: Solid State Phys.* **3** 285

[17] Spanjaard D, Guillot C, Desjonquères M C, Treglia G and Lecante J 1985 *Surf. Sci. Rep.* **5** 1

[18] Thiele J, Guillot C, Barrett N T, Belkhou R and Baudoing-Savois R 1994 *J. Physique* at press

[19] Belkhou R, Barrett N T, Guillot C, Fang M, Barbier A, Eugène J, Carrière B, Naumovic D and Osterwalder J 1993 *Surf. Sci.* **297** 40

[20] Barrett N T, Senhaji A, Belkhou R, Guillot C, Legrand B and Tréglia G 1994 *J. Electron. Spectrosc. Relat. Phenom.*